

# **MICROCRACK PROPAGATION UNDER THERMAL SHOCK**

By  
Vaughn Anderson  
Hasan Demirkoparan  
Can Mavruk

## **ABSTRACT**

The propagation of a pre-existing crack in a finite solid cylinder subjected to thermal shock has been studied. We are interested in predicting the reliability of rocket propellants subject to temperature cycling over time. We assume that propellant is a brittle material and can be modeled as elastic until the point of failure or cracking. We demonstrate a method of computing the stress history of a finite cylinder from its temperature history. The propagation of a Mode-I crack is studied. From an initial crack length, crack geometry, and placement, we determine the stress intensity factor and hence the magnitude of thermal shock necessary for crack propagation. Our goal is to be able to derive the stress history and resulting crack growth from the temperature history so as to estimate the structural integrity non-destructively.

Work done for Instrumented Sensor Technology (IST) under the direction of Rodney J. Lambert, in partial fulfillment of the requirements of Michigan State University MTH 844, and advised by Professor Eldon D. Case.

# Table of Contents

List of Notation .....	3
1. Introduction .....	4
2. Analysis .....	4
Modeling the temperature distribution .....	4
Computing the thermal stresses.....	6
Stress Intensity Factor .....	8
3. Results .....	10
4. Recommendations .....	12
5. Future Work .....	15
6. References .....	16
Appendix A. Heat Diffusion Model.....	18
Appendix B. Heat Diffusion with Convective Cooling on the Boundary .....	20
Appendix C. Finite Difference Method .....	21
Appendix D. Stress-Strain Equations .....	23
Cartesian Coordinates.....	23
Cylindrical Coordinates.....	24
Finite Cylinder.....	25
Appendix E. Conformal Mapping to Determine Stress Intensity Factor .....	30

## List of Notation

$a$	<i>short crack length</i>	$\hat{K}_{\max}$	<i>maximum normalized stress</i>
$a'$	<i>crack length in the cylinder</i>	$R$	<i>radius of infinite cylinder</i>
$A$	<i>heated surface area</i>	$T$	<i>internal temperature distribution</i>
$Bi$	<i>Biot modulus</i>	$\hat{T}$	<i>estimated temperature</i>
$c$	<i>specific heat</i>	$T_{\infty}$	<i>exterior temperature</i>
$\partial_{\hat{n}}$	<i>normal derivative</i>	$\Delta T$	<i>temperature differential</i>
$E$	<i>elastic modulus</i>	$u$	<i>normalized temperature distribution</i>
$G$	<i>shear modulus</i>	$V$	<i>volume of the specimen</i>
$h$	<i>heat transfer coefficient</i>	$\varepsilon$	<i>strain tensor</i>
$\hat{h}$	<i>estimated heat transfer coefficient</i>	$\rho$	<i>density</i>
$H$	<i>half height of cylinder</i>	$dA$	<i>surface element</i>
$J_0$	<i>Bessel's function of order zero</i>	$\sigma$	<i>stress tensor</i>
$J_1$	<i>Bessel's function of order one</i>	$\bar{\sigma}$	<i>normalized stress tensor</i>
$k$	<i>thermal conductivity</i>	$\nu$	<i>Poisson's ratio</i>
$K$	<i>stress intensity</i>	$\alpha$	<i>coefficient of thermal expansion</i>
$\hat{K}_I$	<i>normalized stress intensity</i>	$\mu_j$	<i>radial eigenfunctions</i>
$K_{IC}$	<i>fracture toughness</i>	$\lambda$	<i>Lamé's constant</i>

## 1. Introduction

Many chemical rockets rely on solid propellants as the source of propulsive energy. A controlled burn of the fuel and oxidizer is key to proper operation of these propellants. This is achieved, in part, by carefully regulating the propellant's burning surface area. A structural flaw in the propellant, such as a crack, can increase the exposed area and cause the rocket thrust-versus-time history to deviate from the intended design. In the extreme case these cracks may propagate throughout the propellant so that, upon ignition, pieces of unconsumed propellant dislodge and cause catastrophic failure of the rocket. It is critical to be able to estimate the fracture state of the propellant, i.e., the number of cracks, the size, and the orientation potentially contribute to the degradation of the rocket. The propagation of cracks is a function of thermal stress and the resulting thermal fatigue due to the temperature cycling it is necessary to determine the propellant's temperature history. *Biggs and Singpurwalla* [4] considered the crack propagation in a rocket propellant. The Biggs-Singpurwalla model has simplistic temperature dependence and no geometric concern, i.e., no strain due to the thermal gradient is included. In this project we also consider thermal stresses.

## 2. Analysis

To model the thermal stresses experienced by the rocket body as it is heated or cooled, we begin by describing the temperature distribution over time using the heat diffusion equation. The stress distribution of the propellant is obtained from the temperature distribution; the stress distribution in turn is used to calculate the stress intensity factor experienced by the largest pre-existing flaw in the material. Throughout we assume that the propellant is a brittle material—that the deformations of the propellant are small enough so that linear elastic fracture mechanics (LEFM) gives an accurate description of the cracking. Our goal is to determine the conditions under which a crack with a particular geometry will grow. We seek to make a conservative estimate of the fitness of the propellant: if the propellant has not experienced *any* thermal conditions promoting cracking growth we deem the rocket to be fit. If environmental thermal cycling causes the cracks to grow, then during the ignition of the propellant, these incremented crack lengths may lead to failures that would not have occurred in the absence of thermal cycling. Thus the problem may be seen in two stages: (1) Do cracks propagate prior to ignition and (2) if cracks do propagate prior to ignition, are they long enough to cause failure during ignition.

### Modeling the temperature distribution

The temperature distribution within a body undergoing conductive flow of heat is accurately modeled using the heat equation. It is simplest if we work with  $u = T - T_\infty$ , the

difference between the temperature at a point inside a body  $T$  and the fixed temperature of the surrounding heat sink or source  $T_\infty$ . The heat equation

$$c\rho \frac{\partial u}{\partial t} = k\nabla^2 u \quad (1)$$

describes the evolution of the temperature distribution inside the body;  $c$  is the specific heat,  $\rho$  is the density, and  $k$  is the thermal conductivity of the material. The solutions of the heat equation are highly sensitive to the imposed boundary conditions. If we assume linear convective cooling, the boundary conditions are expressed as

$$k\partial_{\hat{n}}u = -hu, \quad (2)$$

where  $h$  is the heat transfer coefficient and  $\partial_{\hat{n}}u$  is the derivative of  $u$  in the outward normal direction to the boundary. In this project we assume that the propellant's shape is a solid cylinder. The solution of the heat equation for a solid cylinder can be found in any standard book on boundary value problems [5]; we give the basic steps of this computation in appendices A and B.

For a particular geometry, e.g. finite cylinder, infinite plate, etc, it is common to express the functional dependence of heat transfer coefficient, thermal conductivity, and dimension in terms of a single dimensionless number: the Biot modulus  $Bi$ . For example, an infinite plate with thickness  $2H$  has Biot modulus  $Bi = hH / k$  while an infinite cylinder of radius  $R$  has Biot modulus  $Bi = hR / k$ . The analytic solutions of the heat equation are determined by the initial temperature distribution and the Biot modulus—a high Biot modulus means that an object is being cooled/heated rapidly relative to its size while a low Biot modulus corresponds to a gradual change in temperature. The damage experienced by a thermally stressed body does not depend solely upon the magnitude of the temperature gradient but critically on the rate at which heat infiltrates or exits the material relative the capacity of the body to distribute it. The Biot modulus is a ratio relating the size and surface heat permeability of the body to its heat conductivity.

The heat transfer coefficient  $h$  can vary by several orders of magnitude with the same cooling medium. For example a metal surface cooling in static air has  $h=0.0011 \text{ W/cm}^2 \text{ K}$  while the same metal surface in moving air has  $h=0.050 \text{ W/cm}^2 \text{ K}$ . The heat transfer coefficient can vary with temperature and may change as the body cools but we will assume that it remains constant throughout.<sup>1</sup>

---

<sup>1</sup> Suppose a specimen is exposed to a fluid at a temperature  $T_\infty$ . The estimated heat transfer coefficient is

We applied a variety of numerical methods to the solution of the heat equation. The finite difference method is simple to implement and gives a reasonable agreement with the analytical solution. We used this technique to find approximate solutions to the heat equation over a finite cylinder (see Appendix C).

### Computing the thermal stresses

The dynamics of a bulk material involve the interplay of two quantities: the stress, which determines the resolution of forces inside the body; and the strain, which is determined by the deformations of the body. The stress in a material is described by a tensor,  $\sigma$ . Given a surface element  $dA$  the stress tensor returns the pressure experienced by the area element. The strain tensor  $\varepsilon$  measures the deformation of the body from its initial configuration.

For small displacements  $(u, v, w)$ , where deformation of the body is given by the map

$$(r, \theta, z) \rightarrow (r + u, \theta + v, z + w), \quad (3)$$

the components of the strain tensor are given by

$$\begin{aligned} \varepsilon_r &= \frac{\partial u}{\partial r}, \quad \varepsilon_\theta = \frac{u}{r} + \frac{1}{r} \frac{\partial v}{\partial \theta}, \quad \varepsilon_z = \frac{\partial w}{\partial z}, \\ \gamma_{r\theta} &= \frac{1}{r} \frac{\partial u}{\partial \theta} + \frac{\partial v}{\partial r} - \frac{v}{r}, \quad \gamma_{\theta z} = \frac{\partial v}{\partial z} + \frac{1}{r} \frac{\partial w}{\partial \theta}, \quad \gamma_{zr} = \frac{\partial u}{\partial z} + \frac{\partial w}{\partial r}. \end{aligned} \quad (4)$$

In linear elastic mechanics Hooke's Law governs the interaction of the stress and strain. Specializing to the case where only thermal stresses are present we get

---


$$\hat{h} = \frac{\rho C_p V}{A(T_\infty - \hat{T})} \frac{d\hat{T}}{dt}$$

where  $V$  is the volume of the specimen,  $T$  is true specimen temperature,  $C_p$  is specific heat of the specimen,  $\rho$  is the density,  $A$  is the heated surface area of the specimen,  $\hat{T}$  is estimated temperature [7]. For a given material at lower quench temperature differences,  $\Delta T$ , estimated surface heat transfer coefficient curves are similar to one another. For selected quench media and particular temperature ranges  $\hat{h}$  is not monotonic, it goes up and down for different temperatures.

$$\begin{aligned}
\varepsilon_r &= \frac{1}{E} [\sigma_r - \nu(\sigma_\theta + \sigma_z)] + \alpha T, \\
\varepsilon_\theta &= \frac{1}{E} [\sigma_\theta - \nu(\sigma_r + \sigma_z)] + \alpha T, \\
\varepsilon_z &= \frac{1}{E} [\sigma_z - \nu(\sigma_r + \sigma_\theta)] + \alpha T,
\end{aligned} \tag{5}$$

where  $E$  is the elastic modulus,  $G$  is the shear modulus, and  $\nu$  is Poisson's ratio. We assume that the propellant is an isotropic and homogenous material and will neglect the shear terms. To solve for the stress we use the fact that as the body undergoes thermal stress it can at any given time be considered static. The resulting equilibrium conditions required that, in the absence of body forces, the stress tensor  $\sigma$  satisfies

$$\begin{aligned}
\frac{\partial \sigma_r}{\partial r} + \frac{\sigma_r - \sigma_\theta}{r} &= 0, \\
\frac{1}{r} \frac{\partial \sigma_\theta}{\partial \theta} &= 0, \\
\frac{\partial \sigma_z}{\partial z} &= 0.
\end{aligned} \tag{6}$$

Inverting Hooke's Law, (5), we derive an expression for stress tensor in terms of the displacements:

$$\begin{aligned}
\sigma_r &= \lambda e + 2G\varepsilon_r - \frac{\alpha ET}{1-2\nu}, \\
\sigma_\theta &= \lambda e + 2G\varepsilon_\theta - \frac{\alpha ET}{1-2\nu}, \\
\sigma_z &= \lambda e + 2G\varepsilon_z - \frac{\alpha ET}{1-2\nu}.
\end{aligned} \tag{7}$$

Above in (7), the quantity  $e$  is defined as

$$e = \varepsilon_r + \varepsilon_\theta + \varepsilon_z = \frac{\partial u}{\partial r} + \frac{u}{r} + \frac{\partial v}{\partial \theta} + \frac{\partial w}{\partial z}, \tag{8}$$

and the strains  $\varepsilon_r$ ,  $\varepsilon_\theta$ , and  $\varepsilon_z$  are as defined above. Substituting into the equilibrium conditions we obtain sufficient conditions to determine the displacement field. Using this method we derive the stress field resulting from a temperature distribution on a finite cylinder (Appendix D); the stress field is found to be

$$\sigma_r = \frac{\alpha E}{1-2\nu} \left( \frac{1}{R^2} \int_0^R rT dr - \frac{1}{r^2} \int_0^r rT dr \right), \tag{9}$$

$$\sigma_{\theta} = \frac{\alpha E}{1-2\nu} \left[ \left( \frac{1}{r^2} \int_0^r rT \, dr - T \right) + \frac{1}{R^2} \int_0^R rT \, dr \right], \quad (10)$$

$$\sigma_z = 0. \quad (11)$$

An important fact about the stress field on the finite cylinder is that stress vanishes in the axial direction. For further information on the mechanics of solid bodies see [11], [12], or [6].

### Stress Intensity Factor

From the stresses distribution over an uncracked body we can determine the strength of the stresses when a crack is present. The stress field in a cracked body is a superposition of the thermal stresses on the uncracked body with a stress field quantifying the redistribution of the stress around the crack. The crack surface is *traction free*—there is no pressure or tension on the crack surface, though there may be stresses parallel to the crack surface. At corners and crack tips there may be singularities in the stress field; in practice there is a small region of plasticity around these singularities where LEFM does not accurately model the material. However, for brittle materials, the plastic zone is sufficiently small such that LEFM gives a reasonable approximation of the mechanics.

The magnitude of a singularity is called the *stress intensity factor*,  $K$ . The growth of a crack depends on the stress intensity factor at the crack tip. Each material has intrinsic fracture toughness  $K_{IC}$  and if the stress intensity  $K$  at a crack tip exceeds the fracture toughness the crack will grow.

The stresses inside a material induce cracking in three distinct loading modes. As illustrated in Figure 1, Mode I is the opening mode, Mode II the shearing mode, and Mode III the opening mode. In thermal stress Mode I is dominant and we shall restrict our analysis to Mode I tearing and assume that the “worst flaw” present in the propellant is a Mode I crack with a specific length and orientation.

The computation of stress intensity factor is not simple. For different geometric configurations of cracks, stress intensity factors are given in [10].

Initially we investigated the stresses experienced by a surface crack under a single cold shock. We chose this starting point for several reasons. Materials are typically stronger under compression than tension. The surface of a cooling body is under tension as the exterior seeks to contract faster than the interior can accommodate.

We now determine the stress intensity factor of a Mode I crack in the cylinder. The starting point for our calculations is the short-crack approximation. Given a crack with length  $a$  in a semi-infinite solid the normalized stress intensity factor is computed as

$$\hat{K}_I \equiv \frac{K_I(1-\nu)}{E\alpha(T_0 - T_\infty)\sqrt{\pi a}}$$

$$= -\frac{2}{\pi} \int_0^1 \frac{\bar{\sigma}(z,t)}{\sqrt{1-(z/a)^2}} \{1.3 - 0.3(z/a)^{5/4}\} d\left(\frac{z}{a}\right), \quad (12)$$

where  $\bar{\sigma}(z,t)$  is the normalized stress.

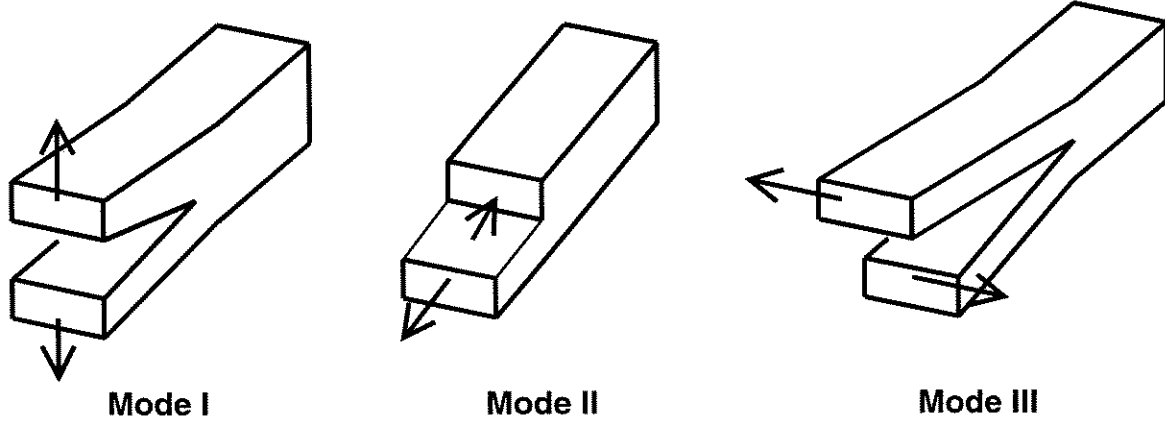


**Figure 1** The three loading modes for a crack

Using a conformal mapping we transform our problem where we have a radial crack in a cylinder to the semi-infinite solid. Using a mapping generated by the conformal transformation  $T$  on the complex plane, where

$$T(z) = \frac{z-1}{z+1}, \quad (13)$$

we can map a circle of unit radius to the half-infinite plane (Figure 2). The thermal stress field on the cylinder maps to a stress field on the infinite plane by the transformation, likewise for the residual stress field. From the conformal mapping we obtain corrections equation for the short-crack stress intensity factor (12) and obtain a function for the stress intensity factor of the cracked cylinder

$$\hat{K}_I = \frac{2}{\pi} \left( \frac{1+a}{1-a} \right) \int_0^1 \frac{\bar{\sigma}_\theta(r,z,t)}{\sqrt{1-(x/a)^2}} \frac{(1-x/a)}{(1+x/a)} \{1.3 - 0.3(x/a)^{5/4}\} d\left(\frac{x}{a}\right) \quad (14)$$

Here  $a$  is the corresponding short crack length given by  $a = a'/(2 - a')$ , where  $a'$  is the crack length in the cylinder.

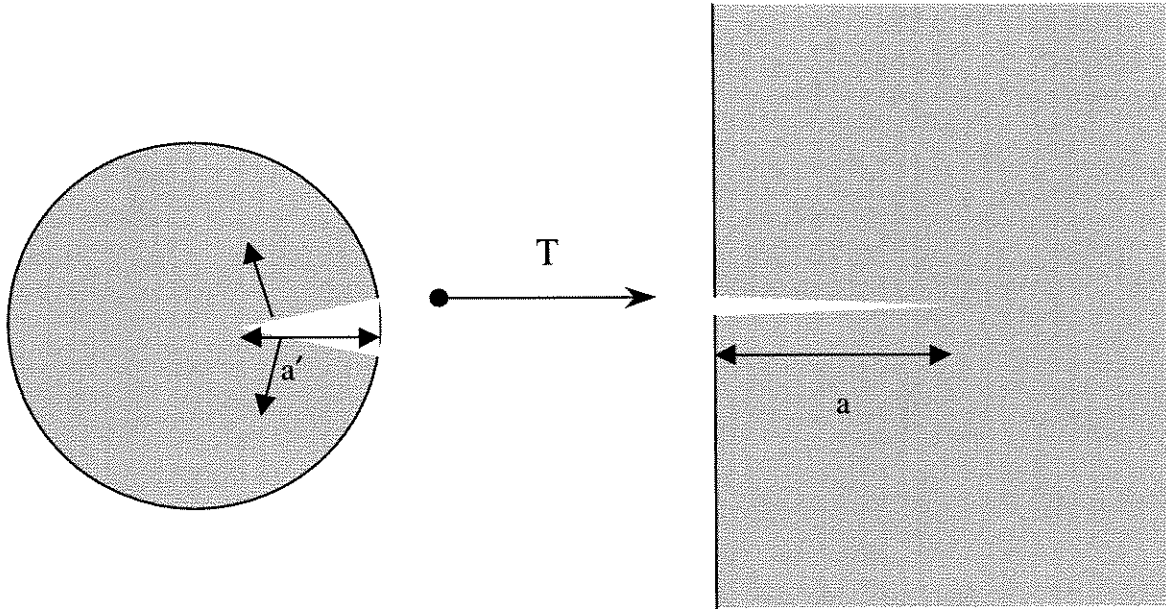


**Figure 2 The conformal mapping transforms the cylindrical crack into a crack in a semi-infinite solid**

There is a corresponding energy model of cracking which uses the strain-energy release rate instead of the stress intensity factor.

### 3. Results

A descriptive picture of the stress history of the propellant as it cools from an initial constant temperature is shown in Figure 3. This diagram shows the stress in the hoop direction. Initially under a cold shock there is a thin layer of tension at the surface with a strong compressive zone inside of the cylinder. The core of the cylinder initially undergoes tension. As cooling continues the stress field is tensile over an outer layer and compressive at the core.

The stresses for the cylinder with traction free surface are much lower than those derived for an infinite plate. Because we consider a finite cylinder there is more freedom for the bulk to expand and contract and the stresses are lower.

Our predictions of the normalized stress intensity factors experienced by radial cracks of various lengths are graphed in Figures 4, 5, and 6. For short cracks the stress intensity quickly peaks and decays. Cracks of sufficient length experience compression under a cold shock event and never grow.

From the graph of the stress intensity factor we determine the conditions under which crack growth can occur. Consider the following example: we are given a cylinder  $H = 3$  m in length and  $R = 0.3$  m in radius made of a material with the following physical properties: density  $\rho = 3$  g/cm<sup>3</sup>, specific heat  $c = 1$  J/g K, thermal conductivity

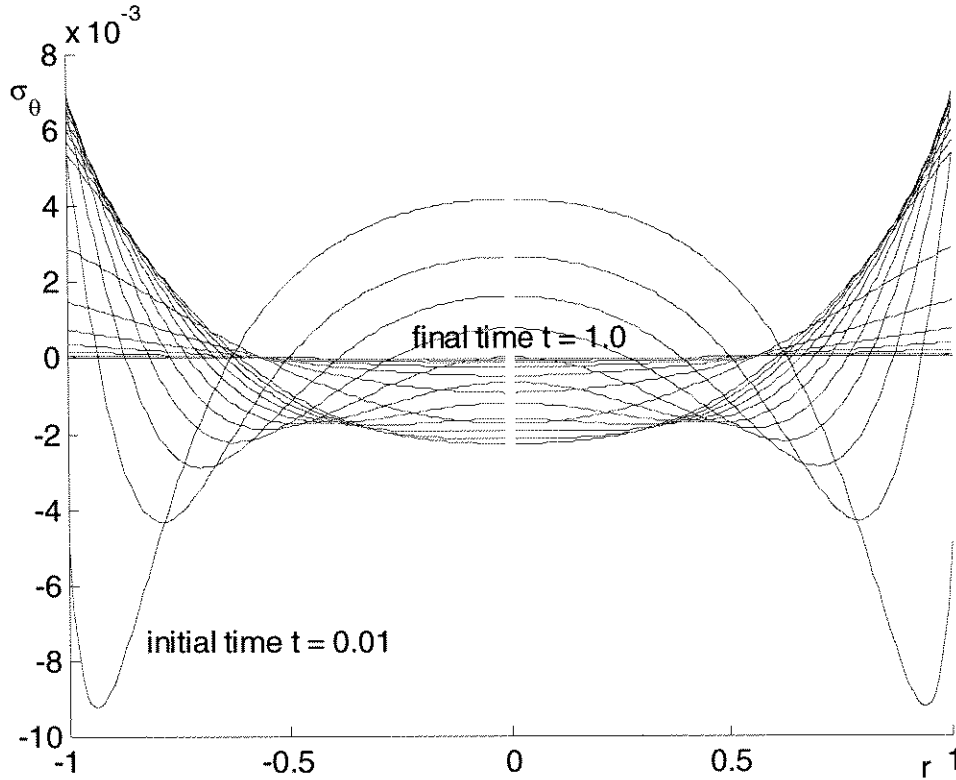


**Figure 3 Stress History in Hoop Direction**

$k = 1.5 \text{ W/cm K}$ , elastic modulus  $E = 5 \text{ GPa}$ , Poisson's ratio  $\nu = 0.3$  and coefficient of thermal expansion  $\alpha = 20 \times 10^{-6} / \text{K}$ . Additionally, we assume that the rocket is being cooled in a strong breeze and the heat transfer coefficient is  $h = 0.05 \text{ J/s cm}^2 \text{ K}$ . The corresponding Biot numbers for this configuration are  $Bi_r = 1.0$  and  $Bi_z = 10.0$ . The fracture strength of the material is estimated to be  $K_{IC} = 1 \text{ MPa m}^{1/2}$ . The fracture strength of most brittle materials is between  $0.5 - 2.0 \text{ MPa m}^{1/2}$ .

From the graph showing the stress intensity factor we see that a short crack will experience the highest normalized stress intensity factor; a crack with length  $0.6 \text{ cm}$  in the cylinder with radius  $30 \text{ cm}$  corresponds to crack length of  $a=0.02$ . The maximum normalized stress factor predicted at the crack tip of this small crack is  $\hat{K}_{\max} = 0.033$ . If we compare the stress intensity factor with the fracture strength we get

$$K_{IC} = \frac{E\alpha \Delta T}{1-2\nu} \hat{K}_{\max}$$

$$1 \text{ MPa m}^{1/2} = \frac{(5 \text{ GPa})(20 \times 10^{-6} / \text{K})\Delta T}{1-2(0.3)} \sqrt{\pi(0.6 \text{ cm})} 0.033,$$

and solving for  $\Delta T$  we find that crack growth occurs for a cold shock of  $\Delta T = 883 \text{ K}$ .

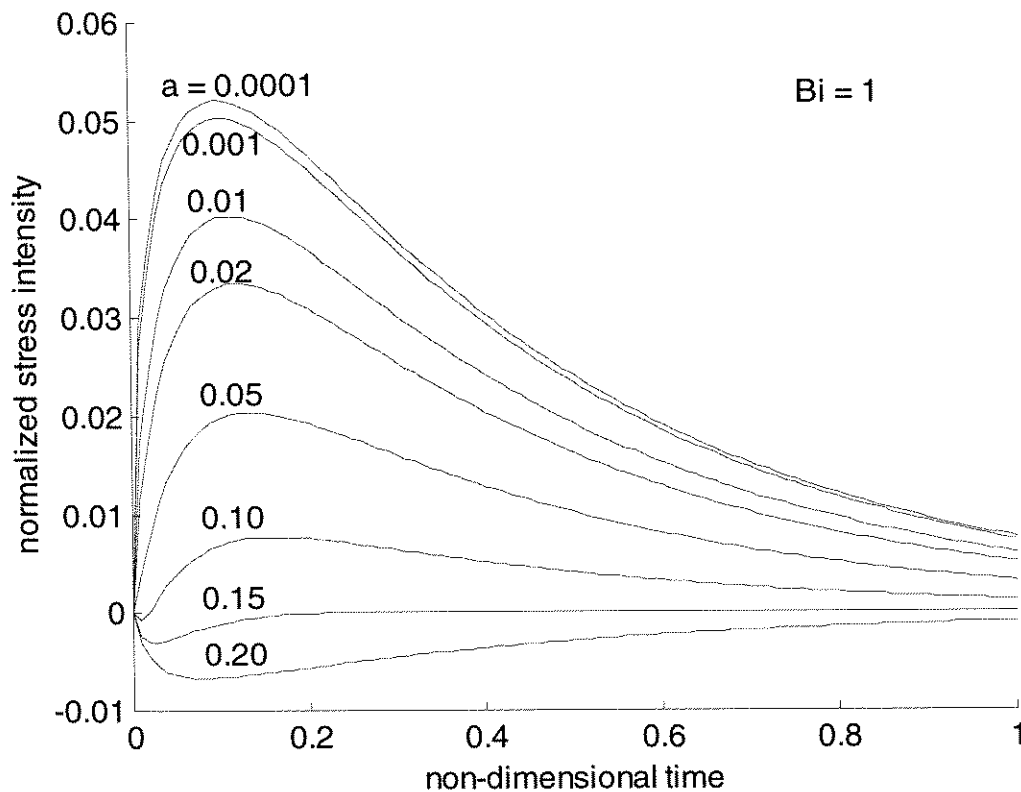


**Figure 4 Stress Intensity Factor,  $Bi = 1$**

The temperatures gradients necessary for crack growth for various Biot moduli are shown in Table 1. Note that the necessary temperature variations for crack growth are an order of magnitude greater than those experienced in the Earth’s most extreme natural environments where temperatures vary by at most 60 degrees Celsius.

#### 4. Recommendations

In our analysis we have studied the growth of cracks in a material subject to temperature shocks common to the natural environment. We have assumed that the rocket propellant is an isotropic, homogenous, brittle material with small pre-existing cracks. Additionally, we have modeled the thermal stress distribution on the body assume that all surfaces are traction free. Unfortunately, our analysis shows that with these assumptions *no* crack growth is likely under the environmental temperature gradients associated with weather and solar exposure. Nevertheless, experience has shown that the rocket does age over time. What then are other possible mechanisms for cracking?

One possibility is that the medium is not isotropic and homogeneous; that the grain sizes of the propellant are a significant factor in determining the stress distribution within the propellant. The stresses are not as smoothly distributed inside a non-

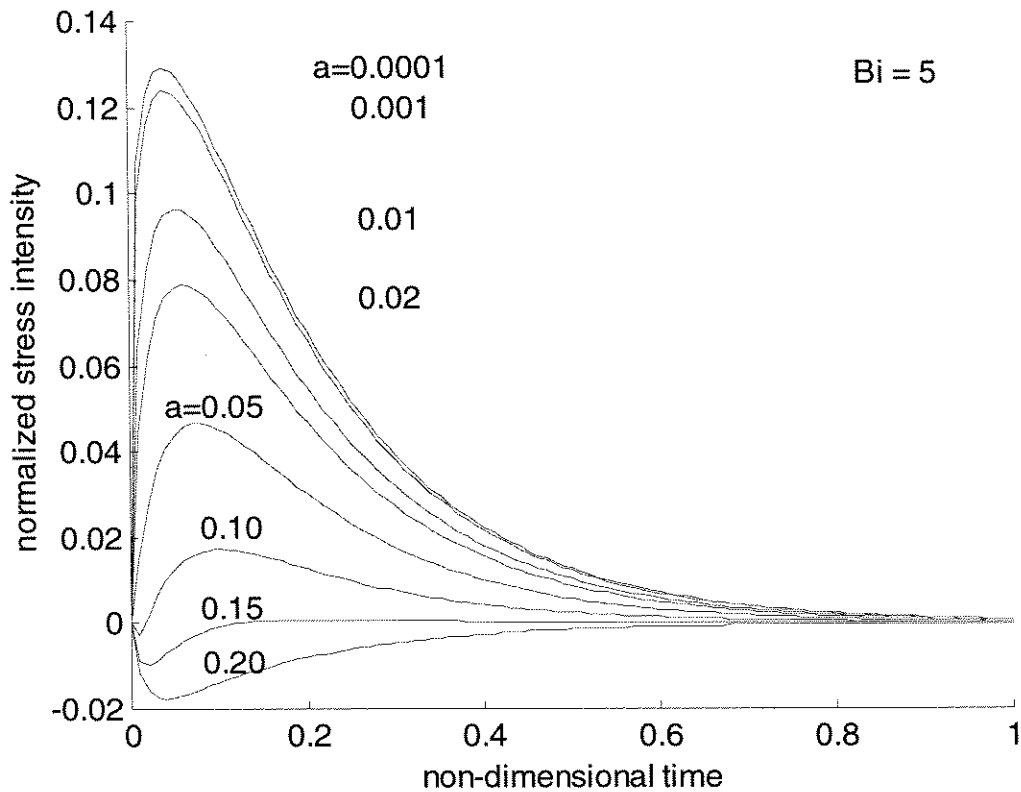


**Figure 5 Stress Intensity Factor,  $Bi = 5$**

homogeneous material; body and stress fractures will thus grow at lower temperature gradients.

In this project we model only the rocket propellant and assume the boundary is free to expand or contract as needed. In practice the rocket propellant is encased in a thin metallic covering; differences in expansion coefficient between the propellant and its case could cause large stresses and introduce stresses at the surface of the propellant.

Another possibility is that the physical properties such as coefficient of thermal expansion  $\alpha$ , the thermal conductivity  $k$ , and the elastic modulus  $E$  may change significantly with temperature. For example, at  $-15^\circ C$  the crystal structure of ice changes; ice is significantly denser below this temperature than above it. This non-linearity in the thermal expansion coefficient results in high stresses present only when crossing a particular temperature value. Perhaps a similar physical change occurs in the propellant as its temperature passes through some specific temperature range.

The dimensions of the propellant cylinder are also significant in crack growth. With increasing size there is a proportional increase of the Biot modulus; a cylinder with twice the diameter has double the Biot modulus. But even a cylinder 4 m in diameter (the same size as the space shuttle's solid rocket booster) would have a Biot modulus of at

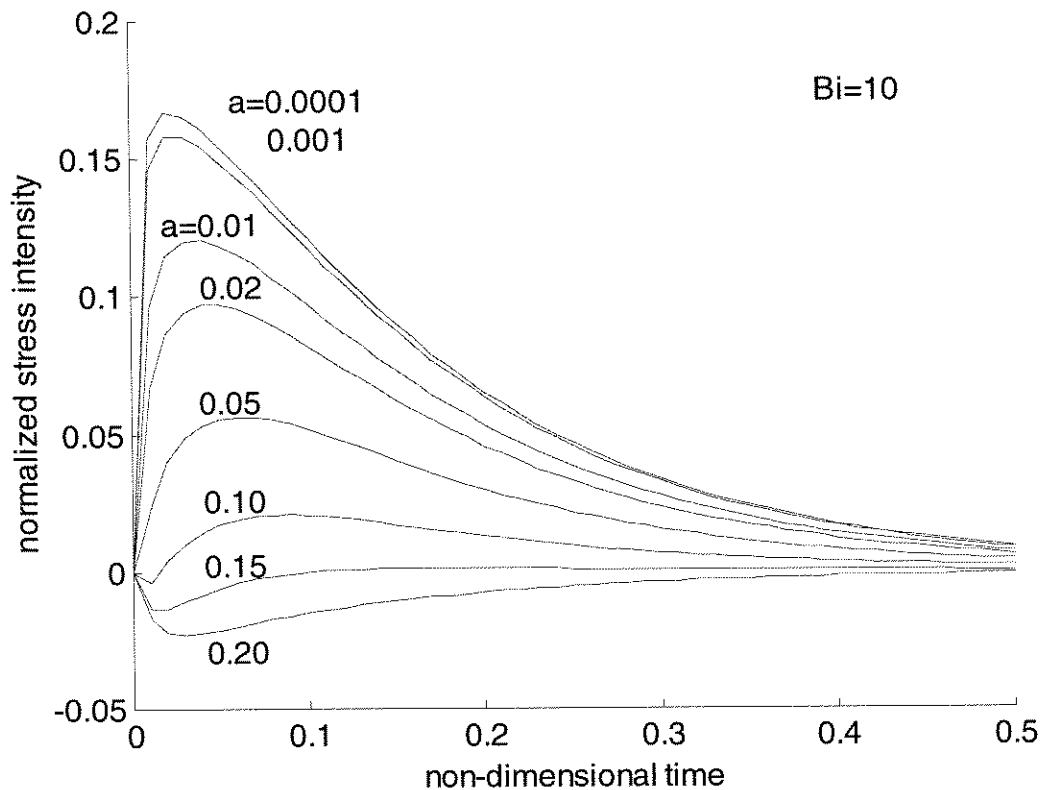


**Figure 6 Stress Intensity Factor,  $Bi = 10$**

most 10 or 20 when cooled in air. The thermal stresses also vary proportional to the size of the body. Additionally with size comes the likelihood of larger flaws; a statistical model of the number and size of flaws present in a material is given by Weibull's statistics [14]. Larger materials are more likely to have large flaws.

Would thermal fatigue appear after several cold/hot cycles? It is possible that damage is done below the level at which the cracks are seen to grow during a single cold shock but which are apparent after repeated temperature cycling. We consider this possibility to be unlikely because thermal fatigue usually occurs for temperature gradients close to that necessary for crack growth [8].

The true test of the rocket is whether the propellant can survive the extreme temperature gradients of ignition and launch without catastrophic cracking leading to engine failure. We can assume that the flaws present in a newly manufactured rocket are highly unlikely to lead to such catastrophic failure. A less conservative bound on rocket fitness based on its thermal history could be obtained by analyzing the problem from two viewpoints: which cracks grow explosively on ignition, and which stress history will produce these cracks in the material.

## 5. Future Work

From these initial calculations of the stress and the stress intensity it is possible to find conditions on the maximum length of the crack formed under cold shock. Two possibilities must be considered: either the stresses are sufficient to penetrate to the core region where a subsequent cold shock event may cause catastrophic failure; or the cracks will be confined to a region near the surface of the cylinder. The effects of heat shock need also be considered as regions which are under compression under cold shock will be under tension at the rocket is reheated. Different crack geometries should also be studied.

There are many possible directions we can pursue in the future once we have finished our study of crack growth using fracture mechanics.

One problem, which has not been well studied, is how to find the stresses on a material when the Biot modulus is no longer assumed to be constant. There are many factors involved in the Biot modulus. As the material is heated or cooled its physical properties and dimensions will change. Typically, the boundary conditions at the interface between the cylinder and its cooling or heating medium will change over time. For example, a hot object quenched in water may cause the water to boil; the conductivity through this boundary can change by several orders of magnitude because the water has changed state! Even if the difference is not so drastic changes in the temperature difference between the cooling medium and the material can produce different boundary conditions. Another example is the difference between cooling in a static medium and cooling in a convective medium.

A second possibility is to apply our understanding of the stresses to the damage mechanics of the model. The geometric modeling of a damage field may give more insights to the conditions under which the material fractures than simply studying the growth of a single crack.

Crack Length (cm)	Normalized Stress Intensity ( $Bi = 1$ )	Normalized Stress Intensity ( $Bi = 5$ )	Normalized Stress Intensity ( $Bi = 10$ )	Cracking Temperature Difference (in K, $Bi = 1$ )	Cracking Temperature (In K, $Bi = 5$ )	Cracking Temperature (In K, $Bi = 10$ )
0.003	0.052	0.129	0.167	7924	3194	2467
0.03	0.050	0.124	0.159	2606	1051	819
0.3	0.040	0.096	0.121	1030	429	341
0.6	0.033	0.079	0.097	883	369	300
1.5	0.020	0.047	0.057	921	392	323
3	0.008	0.017	0.021	1629	766	620
4.5	0.001	0.001	0.002	10638	10638	5319
6	-0.007	-0.018	-0.023	-1316	-512	-401

**Table 1 Cracking Temperatures for cracks of various lengths**

## 6. References

- [1] T.J. Lu and N. A. Fleck, "The thermal shock resistance of solids," *Acta Mater*, vol. 46, pp 4755-4768, 1998.
- [2] L. T. Zhao, T.J. Lu and N. A. Fleck, "Crack channeling and spalling in a plate due to thermal shock loading," *J. Mech. Phys Solids*, vol. 48, pp 867-897, 2000.
- [3] C. M. Cheng, "Resistance to thermal shock," *J. Am. Rocket Soc.*, vol. 21, pp 147-153, 1951.
- [4] G. L. Biggs and N. D. Singpurwalla, "Predicting reliability of Rocket Propellants over time," [To appear].
- [5] R. B. Guenther and J. W. Lee, *Partial Differential Equations of Mathematical Physics and Integral Equations*, New York: Dover Publications, Inc., 1996, pp. 364-367.
- [6] Z. Zudans, T. C. Yen and W. H. Steigelmann, *Thermal Stress Techniques in the Nuclear Industry*, New York: American Elsevier Publishing Company, Inc., 1965, pp 202-234.
- [7] Y. Kim, W. -J. Lee and E. D. Case, "The measurement of the surface heat transfer coefficient for ceramics quenched into a water bath," *Materials Science and Engineering*, A145, pp L7-L11, 1991.
- [8] E. D. Case, "The saturation of thermomechanical fatigue damage in brittle materials", [To appear].
- [9] R. B. Hertzberg, *Deformation and Fracture Mechanics of Engineering Materials*, New York: John Wiley and Sons, 1989, pp 277-278.

- [10] H. Tada, P. C. Paris and G. R. Irwin, *The Stress Analysis of Cracks Handbook*, New York: The American Society of Mechanical Engineers, 2000.
- [11] S. Timoshenko and J. N. Goodier, *Theory of Elasticity*, New York: McGraw-Hill, 1951.
- [12] M. F. Kanninen and C. H. Popelar, *Advanced Fracture Mechanics*, New York: Oxford Science Publications, 1985.
- [13] W. P. Rogers, Ashley F. Emery, Richard C. Bradt, and Albert S. Kobayashi, "Statistical Study of Thermal Fracture of Ceramic Materials in the Water Quench Test," *J. Am. Ceram. Soc.*, vol. 70, no. 6, pp 406-412, 1987.
- [14] S. S. Manson and R. W. Smith, "Theory of Thermal Shock Resistance of Brittle Materials Based on Weibull's Statistical Theory of Strength" *J. Am. Ceram. Soc.*, vol. 38, no. 1, pp 18-27, 1955.

## Appendix A. Heat Diffusion Model

To find the temperature inside the solid cylinder  $x^2 + y^2 \leq \alpha^2$ ,  $0 \leq z \leq b$ , with the given boundary condition:  $u = 0$  on the three sides of the cylinder and initially  $u = f(r, z)$ ,  $r = \sqrt{x^2 + y^2}$  is a given radially symmetric function, we need to solve following pde:

$$\begin{aligned} u_t &= a \Delta u, \quad x \in D, \quad t > 0, \\ u(x, t) &= 0, \quad x \in B, \quad t \geq 0, \\ u(x, 0) &= f(x), \quad x \in \bar{D}, \end{aligned} \quad (15)$$

where  $D$  is the cylinder and  $B$  its bounding surface. By using separation of variables with  $u(x, t) = v(x)T(t)$ , we have following eigenvalue problem:

$$\begin{aligned} \Delta v - cv &= 0, \quad x \in D, \\ v &= 0, \quad x \in B, \end{aligned} \quad (16)$$

and the time equation

$$T' - acT = 0, \quad t > 0, \quad (17)$$

where  $c$  is again the separation constant.

For nontrivial solutions of (15), we need to set  $c = \lambda^2$  with  $\lambda > 0$ . In view of the radial symmetry of  $f$  we seek a radially symmetric solution  $u$ . Then  $v$  will be radially symmetric,  $v = v(r, z)$  in cylindrical coordinates and equation (15) can be written as

$$\begin{aligned} \frac{1}{r} \frac{\partial}{\partial r} \left( r \frac{\partial v}{\partial r} \right) + \frac{\partial^2 v}{\partial z^2} + \lambda^2 v &= 0, \quad (r, z) \in D, \\ v(r, z) &= 0, \quad (r, z) \in B. \end{aligned} \quad (18)$$

By using separation of variables one more time with  $v(r, z) = R(r)Z(z)$ , we get

$$\frac{1}{r} (rR')'Z + RZ'' + \lambda^2 RZ = 0, \quad (19)$$

and, upon separating variables,

$$\frac{1}{r} (rR')' - \tilde{c}R = 0, \quad R(\alpha) = 0, \quad (20)$$

together with

$$Z'' + (\lambda^2 + \tilde{c})Z = 0, \quad Z(0) = Z(b) = 0. \quad (21)$$

Equation (20) can have nontrivial solutions only if  $\tilde{c} < 0$ , say  $\tilde{c} = -\nu^2$ , with  $\nu > 0$ .

Note that the differential equation in (20), which we now express as

$$R'' + \frac{1}{r}R' + \nu^2 R = 0, \quad (22)$$

is singular when  $r = 0$ , but physically meaningful solutions must be twice continuously differentiable in  $0 \leq r \leq \alpha$ . Equation (22) is Bessel's equation and has only one bounded solution (up to constant multiples)  $R(r) = J_0(\nu r)$ , where  $J_0(z)$  is Bessel's function of order zero. To satisfy boundary condition in (3), we require that  $R(r) = J_0(\nu r) = 0$ . Thus, if  $\mu_1 < \mu_2 < \dots < \mu_n < \dots$  are the positive zeros of  $J_0(z)$ , we must choose  $\nu = \nu_j = \frac{r_j}{\alpha}$ .

In summary, solution to original problem is given by

$$u(r, z, t) = \sum_{j,n=1}^{\infty} c_{jn} \exp\left(-\frac{a\mu_j^2 t}{\alpha}\right) \exp\left(-\frac{n^2\pi^2}{b^2}at\right) J_0\left(\frac{\mu_j r}{\alpha}\right) \sin\left(\frac{n\pi z}{b}\right), \quad (23)$$

with the coefficients given by

$$c_{pq} = \frac{4}{\alpha^2 b J_1^2(\mu_p)} \int_0^{\alpha} \int_0^b f(r, z) r J_0\left(\frac{\mu_p r}{\alpha}\right) \sin\left(\frac{q\pi z}{b}\right) dr dz. \quad (24)$$

A more detailed explanation of how separation of variables to solve the heat equation in the cylindrical symmetric coordinates is found in [5].

## Appendix B. Heat Diffusion with Convective Cooling on the Boundary

As a further assumption we can solve the heat equation with convective cooling on the boundary. Convective cooling is represented by the boundary conditions [6]

$$\begin{aligned} k \frac{\partial u}{\partial r} &= -h_r(T - T_\infty), \quad \text{at } r = \alpha \\ k \frac{\partial u}{\partial z} &= -h_z(T - T_\infty), \quad \text{at } z = \pm \frac{b}{2}, \end{aligned} \quad (25)$$

where  $h_r$  and  $h_z$  may or may not be equal. Applying separation of variables the solution of the heat equation

$$u_t = k \nabla^2 u \quad (26)$$

continues as before; we write  $u(r, z) = R(r)Z(z)$  and as before find that  $R(r) = J_0(\mu r)$  and  $Z(z) = \cos(\mu z)$  Imposing the boundary conditions (25) on the solution we see that

$$u(r, z) = \sum_{j,n=1}^{\infty} c_{jn} \exp\left[-\left(\frac{\mu_j^2}{\alpha^2} + \frac{\gamma_n^2}{b^2}\right)kt\right] \cos(\gamma_n z / b) J_0(\mu_j r / \alpha) \quad (27)$$

where  $\mu_j$  are the roots of

$$\mu_j \frac{J_1(\mu_j)}{J_0(\mu_j)} = Bi_r, \quad (28)$$

with  $Bi_r = h\alpha/k$  the Biot number in the radial direction and  $\gamma_n$  are the roots of

$$\gamma_n \tan \gamma_n = Bi_z, \quad (29)$$

and  $Bi_z = hb/k$  is the Biot number in the axial direction. The coefficients  $c_{jn}$  are given by

$$c_{jn} = \frac{2}{\alpha^2 [J_1^2(\mu_j) + J_0^2(\mu_j)]} \frac{\xi_n}{b(\xi_n + \sin \xi_n \cos \xi_n)} \int_0^\alpha \int_{-b}^b f(r, z) r J_0\left(\frac{\mu_j r}{R}\right) \cos\left(\frac{\xi_n z}{b}\right) dr dz. \quad (30)$$

## Appendix C. Finite Difference Method

One possible numerical approach to modeling the solutions of the heat equation is linear difference equations. In this appendix we apply this technique to solving the heat equation over a finite cylinder.

To begin with we choose a set of points at which we will estimate the temperature and the evolution of temperature over time. Considering first a finite cylinder we assume a radially symmetric solution  $u(r, z, t)$  as in the previous appendix. We choose to follow the evolution of  $u$  at the grid points  $(r_i, z_j)$  over the cylinder of height  $H$  and radius  $R$ , where we subdivide into an  $M \times N$  grid giving,

$$r_0 = 0, r_1 = R/M, r_2 = 2R/M, \dots, r_M = R \quad (31)$$

and

$$z_0 = 0, z_1 = H/N, z_2 = 2H/N, \dots, z_N = H. \quad (32)$$

Additionally we wish to divide time into equal subintervals with  $t_k = k\Delta t$ .

Define  $u_{ij}^{(k)} = u(r_i, z_j, t_k)$ . We wish to approximate the operators in the heat equation

$$\frac{\partial u}{\partial t} = \frac{1}{k} \nabla^2 u \quad (33)$$

using differences instead of differential operators. In cylindrical coordinates the Laplacian  $\nabla^2$  is written

$$\frac{\partial^2}{\partial r^2} + \frac{1}{r} \frac{\partial}{\partial r} + \frac{1}{r^2} \frac{\partial^2}{\partial \theta^2} + \frac{\partial^2}{\partial z^2}, \quad (34)$$

(we can ignore the  $\theta$  component because we are assuming our solutions are radially symmetric). We approximate each differential operator as follows:

$$\frac{\partial^2 u}{\partial r^2}(r_i, z_j, t_k) \approx \frac{1}{[\Delta r]^2} (u_{i+1,j}^{(k)} - 2u_{ij}^{(k)} + u_{i-1,j}^{(k)}), \quad (35)$$

$$\frac{\partial u}{\partial r}(r_i, z_j, t_k) \approx \frac{1}{2[\Delta r]} (u_{i+1,j}^{(k)} - u_{i-1,j}^{(k)}), \quad (36)$$

and

$$\frac{\partial^2 u}{\partial z^2}(r_i, z_j, t_k) \approx \frac{1}{[\Delta z]^2} (u_{i,j+1}^{(k)} - 2u_{ij}^{(k)} + u_{i,j-1}^{(k)}). \quad (37)$$

The heat equation becomes

$$u_{ij}^{(k+1)} = u_{ij}^{(k)} + \frac{\Delta t}{[\Delta r]^2} (u_{i+1,j}^{(k)} - 2u_{ij}^{(k)} + u_{i-1,j}^{(k)}) + \frac{\Delta t}{2r\Delta r} (u_{i+1,j}^{(k)} - u_{i-1,j}^{(k)}) + \frac{\Delta t}{[\Delta z]^2} (u_{i,j+1}^{(k)} - 2u_{ij}^{(k)} + u_{i,j-1}^{(k)}). \quad (38)$$

## Appendix D. Stress-Strain Equations

### Cartesian Coordinates

The thermo elastic strain  $\varepsilon$  consists of two parts: one component related to stress by Hooke's law and another resulting from free thermal expansion. These relations are

$$\begin{aligned}
 \varepsilon_x &= \frac{1}{E} [\sigma_x - \nu(\sigma_y + \sigma_z)] + \alpha T, \\
 \varepsilon_y &= \frac{1}{E} [\sigma_y - \nu(\sigma_x + \sigma_z)] + \alpha T, \\
 \varepsilon_z &= \frac{1}{E} [\sigma_z - \nu(\sigma_x + \sigma_y)] + \alpha T, \\
 \gamma_{xy} &= \frac{1}{G} \tau_{xy}, \quad \gamma_{yz} = \frac{1}{G} \tau_{yz}, \quad \gamma_{zx} = \frac{1}{G} \tau_{zx},
 \end{aligned} \tag{39}$$

where  $\alpha$  is the coefficient of thermal expansion,  $T$  is the temperature change with respect to reference temperature, and the shear modulus  $G$  is related to the modulus of elasticity  $E$  and Poisson's ratio  $\nu$  by

$$G = \frac{E}{2(1+\nu)}. \tag{40}$$

The strain components are related to the deformations  $u$ ,  $v$ , and  $w$  in the  $x$ -,  $y$ -, and  $z$ -directions, respectively, by

$$\begin{aligned}
 \varepsilon_x &= \frac{\partial u}{\partial x}, \quad \varepsilon_y = \frac{\partial v}{\partial y}, \quad \varepsilon_z = \frac{\partial w}{\partial z}, \\
 \gamma_{xy} &= \frac{\partial u}{\partial y} + \frac{\partial v}{\partial x}, \quad \gamma_{yz} = \frac{\partial u}{\partial z} + \frac{\partial w}{\partial y}, \quad \gamma_{zx} = \frac{\partial w}{\partial x} + \frac{\partial u}{\partial z}.
 \end{aligned} \tag{41}$$

By solving for the stresses, equations 3.1 can be written alternatively as

$$\begin{aligned}
 \sigma_x &= \lambda e + 2G\varepsilon_x - \frac{\alpha ET}{1-2\nu}, \\
 \sigma_y &= \lambda e + 2G\varepsilon_y - \frac{\alpha ET}{1-2\nu}, \\
 \sigma_z &= \lambda e + 2G\varepsilon_z - \frac{\alpha ET}{1-2\nu}, \\
 \tau_{xy} &= G\gamma_{xy}, \quad \tau_{yz} = G\gamma_{yz}, \quad \tau_{zx} = G\gamma_{zx},
 \end{aligned} \tag{42}$$

where

$$\lambda = \frac{\nu E}{(1+\nu)(1-2\nu)} \quad (43)$$

is Lamé's constant and

$$\varepsilon = \varepsilon_x + \varepsilon_y + \varepsilon_z = \frac{\partial u}{\partial x} + \frac{\partial v}{\partial y} + \frac{\partial w}{\partial z} \quad (44)$$

is the volumetric dilatation, i.e., the change of volume per unit volume.

### Cylindrical Coordinates

The strain components in terms of displacements  $u$ ,  $v$ , and  $w$  in the radial, tangential and axial directions respectively are given by

$$\begin{aligned} \varepsilon_r &= \frac{\partial u}{\partial r}, \quad \varepsilon_\theta = \frac{u}{r} + \frac{1}{r} \frac{\partial v}{\partial \theta}, \quad \varepsilon_z = \frac{\partial w}{\partial z}, \\ \gamma_{r\theta} &= \frac{1}{r} \frac{\partial u}{\partial \theta} + \frac{\partial v}{\partial r} - \frac{v}{r}, \quad \gamma_{\theta z} = \frac{\partial v}{\partial z} + \frac{1}{r} \frac{\partial w}{\partial \theta}, \quad \gamma_{zr} = \frac{\partial u}{\partial z} + \frac{\partial w}{\partial r}. \end{aligned} \quad (45)$$

Then stress-strain relations in cylindrical coordinates are

$$\begin{aligned} \varepsilon_r &= \frac{1}{E} [\sigma_r - \nu(\sigma_\theta + \sigma_z)] + \alpha T, \\ \varepsilon_\theta &= \frac{1}{E} [\sigma_\theta - \nu(\sigma_r + \sigma_z)] + \alpha T, \\ \varepsilon_z &= \frac{1}{E} [\sigma_z - \nu(\sigma_r + \sigma_\theta)] + \alpha T. \end{aligned} \quad (46)$$

By assuming temperature distribution is a function of radial distance  $r$  only and  $\varepsilon_z = 0$  throughout the cylinder, and the lateral surface of the cylinder is traction free, i.e.,  $\sigma_r = 0$  at  $r = b$ , for an infinite solid cylinder, we get

$$\begin{aligned}
u &= \frac{1+\nu}{1-\nu} \frac{\alpha}{r} \left[ (1-2\nu) \frac{r^2}{b^2} \int_0^b Tr dr + \int_0^r Tr dr \right], \\
\sigma_r &= \frac{E\alpha}{1-\nu} \left[ \frac{1}{b^2} \int_0^b Tr dr - \frac{1}{r^2} \int_0^r Tr dr \right], \\
\sigma_\theta &= \frac{E\alpha}{1-\nu} \left[ \frac{1}{b^2} \int_0^b Tr dr + \frac{1}{r^2} \int_0^r Tr dr - T \right], \\
\sigma_z &= \frac{E\alpha}{1-\nu} \left[ \frac{2\nu}{b^2} \int_0^b Tr dr - T \right].
\end{aligned} \tag{47}$$

For more detailed derivations of these formulas see [6].

### Finite Cylinder

To solve for the stresses on a finite cylinder we begin with Hooke's Law in cylindrical coordinates (46). Solving for the stresses  $\sigma_r$ ,  $\sigma_\theta$ , and  $\sigma_z$  in terms of the strains  $\varepsilon_r$ ,  $\varepsilon_\theta$ , and  $\varepsilon_z$  gives

$$\begin{aligned}
\sigma_r &= \lambda e + 2G\varepsilon_r - \frac{\alpha ET}{1-2\nu}, \\
\sigma_\theta &= \lambda e + 2G\varepsilon_\theta - \frac{\alpha ET}{1-2\nu}, \\
\sigma_z &= \lambda e + 2G\varepsilon_z - \frac{\alpha ET}{1-2\nu}.
\end{aligned} \tag{48}$$

In cylindrical coordinates we have

$$e = \varepsilon_r + \varepsilon_\theta + \varepsilon_z = \frac{\partial u}{\partial r} + \frac{u}{r} + \frac{\partial v}{\partial \theta} + \frac{\partial w}{\partial z}. \tag{49}$$

The equilibrium equations in the absence of body forces are

$$\begin{aligned}
\frac{\partial \sigma_r}{\partial r} + \frac{\sigma_r - \sigma_\theta}{r} &= 0, \\
\frac{1}{r} \frac{\partial \sigma_\theta}{\partial \theta} &= 0, \\
\frac{\partial \sigma_z}{\partial z} &= 0.
\end{aligned} \tag{50}$$

If we substitute for  $\sigma_r$  and  $\sigma_\theta$  in the first equation of (50) above we get

$$\frac{\partial}{\partial r} \left( \lambda e + 2G \varepsilon_r - \frac{\alpha E T}{1-2\nu} \right) + \frac{2G}{r} (\varepsilon_r - \varepsilon_\theta) = 0. \quad (51)$$

We can further reduce this equation so it involves only the displacements  $u$ ,  $v$ , and  $w$  in the  $r$ ,  $\theta$ , and  $z$ -directions, respectively, giving

$$\lambda \left( \frac{\partial^2 u}{\partial r^2} + \frac{\partial}{\partial r} \left[ \frac{u}{r} + \frac{\partial v}{\partial \theta} \right] + \frac{\partial^2 w}{\partial r \partial z} \right) + 2G \frac{\partial^2 u}{\partial r^2} - \frac{\alpha E}{1-2\nu} \frac{\partial T}{\partial r} + \frac{2G}{r} \left( \frac{\partial u}{\partial r} - \frac{u}{r} - \frac{\partial v}{\partial \theta} \right) = 0. \quad (52)$$

Assuming that the displacement in  $\theta$ -direction vanishes we get

$$(\lambda + 2G) \left[ \frac{\partial^2 u}{\partial r^2} + \frac{1}{r} \frac{\partial u}{\partial r} - \frac{1}{r^2} u \right] + \lambda \frac{\partial^2 w}{\partial r \partial z} = \frac{\alpha E}{1-2\nu} \frac{\partial T}{\partial r}. \quad (53)$$

Using the fact that

$$\frac{\partial^2 u}{\partial r^2} + \frac{1}{r} \frac{\partial u}{\partial r} - \frac{1}{r^2} u = \frac{\partial}{\partial r} \left( \frac{1}{r} \frac{\partial}{\partial r} [ru] \right), \quad (54)$$

we integrate (53) to get

$$(\lambda + 2G) \frac{1}{r} \frac{\partial (ru)}{\partial r} + \lambda \frac{\partial w}{\partial z} = \frac{\alpha E}{1-2\nu} T + C_1. \quad (55)$$

Similarly we substitute for  $\sigma_z$  in the last equation of (50) to find the displacement in the  $z$ -direction

$$\frac{\partial}{\partial z} \left( \lambda e + 2G \varepsilon_z - \frac{\alpha E T}{1-2\nu} \right) = 0, \quad (56)$$

or

$$\lambda \frac{1}{r} \frac{\partial^2 (ru)}{\partial z \partial r} + (\lambda + 2G) \frac{\partial^2 w}{\partial z^2} = \frac{\alpha E}{1-2\nu} \frac{\partial T}{\partial z}. \quad (57)$$

Integrating this equation gives

$$\lambda \frac{1}{r} \frac{\partial (ru)}{\partial r} + (\lambda + 2G) \frac{\partial w}{\partial z} = \frac{\alpha E}{1-2\nu} T + C_2. \quad (58)$$

Equations (55) and (58) form a system of first order differential equations for the displacements. Using linear algebra we can separate these equations to get two ordinary differential equations depending, which we can solve:

As the stress must vanish at the ends of the cylinder we get that  $C_1 + 2C_2 = 0$ . *The stress vanishes in axial direction!* We can use these conditions to solve for the constants  $C_1$  and  $C_2$  to obtain

$$C_1 = \frac{2}{5} \frac{\alpha E}{1-2\nu} \frac{1}{R^2} \int_0^R rT dr \quad (66)$$

and

$$C_2 = \frac{1}{5} \frac{\alpha E}{1-2\nu} \frac{1}{R^2} \int_0^R rT dr. \quad (67)$$

In the hoop or  $\theta$ -direction the stress becomes

$$\begin{aligned} \sigma_\theta &= \frac{\lambda}{\lambda+G} \frac{\alpha E}{1-2\nu} T + C_1 + C_2 + \frac{G}{\lambda+G} \frac{\alpha E}{1-2\nu} \frac{1}{r^2} \int_0^r rT dr + C_1 - \frac{\alpha E}{1-2\nu} T \\ &= \frac{\alpha E}{1-2\nu} \left[ \left( \frac{1}{r^2} \int_0^r rT dr - T \right) + \frac{1}{R^2} \int_0^R rT dr \right]. \end{aligned} \quad (68)$$

The solution for the stress on the finite cylinder is the same as for an infinite cylinder except the leading constant is  $\alpha E/(1-2\nu)$  instead of  $\alpha E/(1-\nu)$  that the stress in the axial direction vanishes.

We now specialize to the thermal stresses experienced by a finite cylinder starting with a uniform temperature  $T_0$  when it is immersed in a bath with temperature  $T_\infty$ . From 0 we see that the solution to the heat equation is

$$u(r, z, t) = \sum_{j,n=1}^{\infty} c_{jn} \exp \left[ - \left( \frac{\mu_j^2}{R} + \frac{n^2 \pi^2}{H^2} \right) at \right] J_0 \left( \frac{\mu_j r}{R} \right) \cos \left( \frac{\xi_n z}{H} \right) \quad (69)$$

where the coefficients  $c_{jn}$  are given by

$$\begin{aligned} c_{jn} &= \frac{2(T_0 - T_\infty)}{R^2 H [J_0^2(\mu_j) + J_1^2(\mu_j)]} \frac{\xi_n}{\xi_n + \sin \xi_n \cos \xi_n} \int_0^R \int_{-H}^H r J_0 \left( \frac{\mu_j r}{R} \right) \cos \left( \frac{\xi_n z}{H} \right) dr dz \\ &= (T_0 - T_\infty) \frac{2}{\mu_j [J_0^2(\mu_j) + J_1^2(\mu_j)]} \frac{2 \sin \xi_n}{\xi_n + \sin \xi_n \cos \xi_n}. \end{aligned} \quad (70)$$

We can separate this function into the product  $u(r, x, t) = (T_0 - T_\infty)R(r)Z(z)$  where

$$R(r) = \sum_{j=1}^{\infty} \exp \left( - \frac{\mu_j^2 at}{R} \right) \frac{2}{\mu_j [J_0^2(\mu_j) + J_1^2(\mu_j)]} J_0 \left( \frac{\mu_j r}{R} \right) \quad (71)$$

and

$$Z(z) = \sum_{j=1}^{\infty} \exp\left(-\frac{\xi_n^2 at}{H}\right) \frac{2 \sin \xi_n}{\xi_n + \sin \xi_n \cos \xi_n} \cos\left(\frac{\xi_n r}{H}\right) \quad (72)$$

Substituting in equation 0 we get

$$\begin{aligned} \sigma_r &= \frac{\alpha E}{1-2\nu} \left( \frac{1}{R^2} \int_0^R r T dr - \frac{1}{r^2} \int_0^r r T dr \right) \\ &= \frac{\alpha E \Delta T}{1-2\nu} Z(z) \left( \frac{1}{R^2} \int_0^R r R(r) dr - \frac{1}{r^2} \int_0^r r R(r) dr \right) \\ &= \frac{\alpha E \Delta T}{1-2\nu} Z(z) \sum_{j=1}^{\infty} \exp\left[-\frac{\mu_j^2}{R} at\right] \frac{2}{\mu_j (J_0^2(\mu_j) + J_1^2(\mu_j))} \left( \frac{J_1(\mu_j)}{\mu_j} - \frac{J_1(\mu_j r/R)}{\mu_j r/R} \right) \end{aligned} \quad (73)$$

Similarly we find the stress in the hoop direction:

$$\begin{aligned} \sigma_\theta &= \frac{\alpha E}{1-2\nu} \left[ \left( \frac{1}{r^2} \int_0^r r T dr - T \right) + \frac{1}{R^2} \int_0^R r T dr \right] \\ &= \frac{\alpha E \Delta T}{1-2\nu} Z(z) \left[ \left( \frac{1}{r^2} \int_0^r r R(r) dr - R(r) \right) + \frac{1}{R^2} \int_0^R r R(r) dr \right] \\ &= \frac{\alpha E \Delta T}{1-2\nu} Z(z) \sum_{j=1}^{\infty} \exp\left[-\frac{\mu_j^2}{R} at\right] \frac{2}{\mu_j (J_0^2(\mu_j) + J_1^2(\mu_j))} \\ &\quad \left( \frac{J_1(\mu_j)}{\mu_j} - J_0(\mu_j r/R) + \frac{J_1(\mu_j r/R)}{\mu_j r/R} \right) \end{aligned} \quad (74)$$

## Appendix E. Conformal Mapping to Determine Stress Intensity Factor

The computation of the stress intensity factor for a perpendicular crack in a semi-infinite solid is given in [10]; this is the *short-crack limit* and is valid for cracks that are very small relative to the dimensions of the cracked body.

We use a conformal mapping to convert between the short crack limit and our situation where we have a crack pointing radially inward to a cylindrical body. The mapping

$$re^{i\theta} = u = \frac{1-w}{1+w} \quad (75)$$

maps the complex half-plane  $\{w \in \mathbb{C} | \Re(w) \geq 0\}$  to the unit circle. A conformal mapping is useful because it preserves angles; the conformal mapping takes the stress field on the cylinder to a stress field on the infinite half-plane. The stress intensity factor of the crack in the cylinder is a multiple of the stress intensity factor for the short crack. Using coordinates  $(x, y)$  on the complex half-plane the map becomes

$$\begin{aligned} r &= \sqrt{\frac{(1-x)^2 + y^2}{(1+x)^2 + y^2}} & x &= \frac{1-r^2}{1+2r \cos \theta + r^2} \\ \theta &= \arctan \frac{2y}{x^2 + y^2 - 1} & y &= \frac{2r \sin \theta}{1+2r \cos \theta + r^2}. \end{aligned} \quad (76)$$

Differential forms transform as

$$dr = \frac{2(x^2 - y^2 - 1) dx + 4xy dy}{\left[ (1-x)^2 + y^2 \right]^{1/2} \left[ (1+x)^2 + y^2 \right]^{1/2}} \quad (77)$$

and

$$d\theta = \frac{-4xy dx + 2(x^2 - y^2 - 1) dy}{(x^2 - y^2 - 1)^2 + 4y^2} \quad (78)$$

while the normal vector to the crack surface transforms as

$$\frac{\partial}{\partial \theta} = xy \frac{\partial}{\partial x} + \left[ \frac{x^2 + y^2 - 1}{2} + y^2 \right] \frac{\partial}{\partial y} \quad (79)$$

The normalized stress  $\bar{\sigma}_\theta = (1-2\nu) / E\alpha \Delta T \sigma_\theta$  on the radial crack maps to the stress field

$$\bar{\sigma}_y = \frac{1-x}{1+x} \bar{\sigma}_\theta \quad (80)$$

on the crack surface.

The normalized stress intensity factor  $\hat{K}_I$  at the tip of the short crack is

$$\begin{aligned} \hat{K}_I &\equiv \frac{K_I(1-\nu)}{E\alpha(T_0 - T_\infty)\sqrt{\pi a}} \\ &= -\frac{2}{\pi} \int_0^1 \frac{\bar{\sigma}(z,t)}{\sqrt{1-(z/a)^2}} \{1.3 - 0.3(z/a)^{5/4}\} d\left(\frac{z}{a}\right) \end{aligned} \quad (81)$$

where  $K_0 = E\alpha(T_0 - T_\infty)\sqrt{\pi a} / (1-\nu)$  is a reference stress intensity factor. Using the conformal mapping we can compute the stress intensity factor at the crack tip of the radial crack in the cylinder as

$$\hat{K}_I = \frac{2}{\pi} \left( \frac{1+a}{1-a} \right)^{1/2} \int_0^1 \frac{\bar{\sigma}_\theta(r,z,t)}{\sqrt{1-(x/a)^2}} \frac{(1-x/a)}{(1+x/a)} \{1.3 - 0.3(x/a)^{5/4}\} d\left(\frac{x}{a}\right) \quad (82)$$

where the crack length  $a = a'/(2-a')$ .